

Mutual Composite Fermion and composite Boson approaches to balanced and imbalanced bilayer quantum Hall systems

Jinwu Ye

Department of Physics, The Pennsylvania State University, University Park, PA, 16802

(February 7, 2020)

We use and extend both Mutual Composite Fermion (MCF) and Composite Boson (CB) approach to study balanced and imbalanced Bi-Layer Quantum Hall systems (BLQH) and make critical comparisons between the two approaches. We find the CB approach is superior to the MCF approach in the BLQH with broken symmetry. By using this CB theory, we are able to put spin and charge degree freedoms in the same footing, explicitly bring out the spin-charge connection and classify all the possible excitations in a systematic way. We first study the balanced BLQH and re-derive many previous results in a simple and transparent way. Then we apply the theory to study imbalanced BLQH in both ordered and disordered side. On the ordered side, we find that as we increase the imbalance, the system supports continuously changing fractional charges, the spin-wave velocity decreases, the meron pair separation stays the same, while the critical in-plane magnetic field for the Commensurate-Incommensurate transition increases. On the disordered side, we find there are two quantum phase transitions from in-coherent disordered state to a Dipolar Lattice phase and then to the interlayer coherent state as we increase the imbalance. A scenario on how different phases are evolved as the distance between the two layers is increased is proposed. The effects of disorders are also briefly mentioned. Our results are compared with previous microscopic Lowest Landau Level calculations and available experimental data. Limitations of the CB approach are also pointed out.

I. INTRODUCTION

Extensive attention has been lavished on Fractional Quantum Hall Effects (FQHE) in multicomponent systems since the pioneering work by Halperin [1]. These components could be the spins of electrons when the Zeeman coupling is very small or layer indices in multilayered system. In particular, spin-polarized Bilayer Quantum Hall systems at total filling factor $\nu_T = 1$ have been under enormous experimental and theoretical investigations over the last decade [2]. When the interlayer separation d is sufficiently large, the bilayer system decouples into two separate compressible $\nu = 1/2$ layers. Earlier experiments exhibited a strong suppression of the tunneling current at low biases [3]. However, when d is smaller than a critical distance d_c , even in the absence of interlayer tunneling, the system undergoes a quantum phase transition into a novel spontaneous interlayer coherent incompressible phase [2]. Recently, at low temperature, with extremely small interlayer tunneling amplitude, Spielman *et al* discovered a very pronounced narrow zero bias peak in this interlayer coherent incompressible state [4]. M. Kellogg *et al* also observed quantized Hall drag resistance at h/e^2 [5].

Starting from Halperin's 111 wavefunction which describes a bi-layer system with N_1 (N_2) electrons in the top (bottom) layer (the total number of electrons is $N = N_1 + N_2$), using various methods, several authors discovered a Neutral Gapless Mode (NGM) with linear dispersion relation $\omega \sim vk$ and that there is a finite temperature Kosterlitz-Thouless (KT) phase transition associated with this NGM [6–8]. By treating the

two layer indices as two pseudo-spin indices, Girvin, MacDonald and collaborators mapped the bilayer system into a Easy Plane Quantum Ferromagnet (EPQFM) [9,10,2]. They established the mapping by projecting the Hamiltonian of the BLQH onto the Lowest Landau Level (LLL) and then using subsequent Hartree-Fock (HF) approximation and gradient expansion (called LLL+HF in the following). In the picture of EPQFM [2], the canonical ensemble with definite $S^z = N_1 - N_2 = 0$ is replaced by Grand canonical ensemble with fluctuating S^z . The relative fluctuation of S^z is at the order of $1/\sqrt{N} \rightarrow 0$ as $N \rightarrow \infty$. By drawing the analogy with superconductivity where canonical ensemble with definite number of Cooper pairs is shown to be equivalent to BCS wavefunction which is a grand canonical ensemble with indefinite number of Cooper pairs, the authors in [9,10,2] argued this trial wavefunction is a good approximation to the exact ground state. The low energy excitations above the ground state is given by an effective 2 + 1 dimensional XY model. There are 4 flavors of topological defects called "merons" which carry fractional charges $\pm 1/2$ and also have \pm vorticities. They have logarithmic divergent self energies and are bound into pairs at low temperature. The lowest energy excitations carry charge $\pm e$ which are a meron pair with opposite vorticity and the same charge. There is a finite temperature phase transition at T_{KT} where bound states of the 4 flavors of merons are broken into free merons. The large longitudinal resistivity ($\sim 1k\Omega$) observed in [4] at very low temperature indicated that these meron pairs are highly mobil. In the presence of small tunneling, they [9,2] found that when the applied in-plane magnetic

field is larger than a critical field $B_{||}^*$, there is a phase transition from a commensurate state to an incommensurate state (C-IC) with broken translational symmetry. When $B > B_{||}^*$, there is a finite temperature KT transition which restores the translation symmetry by means of dislocations in the domain wall structure in the incommensurate phase. Starting from the EPQFM approach, several groups investigated $I-V$ curves in the presence of small tunneling [11]. In addition to the work mentioned above, there are also many other works done on BLQH. For example, several authors applied different versions of composite fermion Chern-Simon theory to study BLQH systems in [12–14], Scarola and Jain investigated the energetics of a class of Composite Fermion wavefunctions in BLQH system at different filling factors [15].

In this paper, we use both Mutual Composite Fermion (MCF) [21–23] and Composite Boson (CF) approaches [27,28] to study balanced and im-balanced BLQH systems. We identify many problems with MCF approach. Then we develop a simple and effective CB theory which naturally avoids all the problems suffered in the MCF approach. The CB theory may also be applied to study the incoherent disordered insulating side and the quantum phase transitions between different ground states. Therefore the CB approach is superior to the MCF approach in the BLQH with broken symmetry. By using this CB theory, we are able to put spin and charge degree freedoms in the same footing, explicitly bring out the spin-charge connection and classify all the possible excitations in a systematic way. We first study the balanced BLQH and re-derive many previous results in a simple and transparent way. We also make detailed comparisons with the EPQFM calculations and point out the limitations of the CB approach. Then we apply the CB theory to study imbalanced BLQH in both ordered and disordered side. On the ordered side, we find that as we increase the imbalance, the system supports continuously changing fractional charges, the spin-wave velocity decreases quadratically, the meron pair separation stays the same, while the critical in-plane magnetic field for the Commensurate-Incommensurate transition increases. On the disordered side, we find there are two quantum phase transitions from in-coherent disordered state to a Dipolar Lattice (DL) phase and then to the interlayer coherent state as we increase the imbalance. We propose the following scenario on how phases are evolved as the distance between the two layers is increased: For balanced BLQH, there are two critical distances $d_{c1} < d_{c2}$. When $0 < d < d_{c1}$, the system is in the interlayer coherent QH state (ILCQH), when $d_{c1} < d < d_{c2}$, the system is in the quantum disordered insulating state (QDIS), there is a second order transition at d_{c1} driven by the quantum fluctuation. When $d_{c2} < d < \infty$, the system becomes two weakly coupled $\nu = 1/2$ Composite Fermion Fermi Liquid (CFFL) state. There is a first order transition at $d = d_{c2}$. We also discuss briefly the effects of

disorders and compare our results with the previous results achieved from the LLL+HF approach and available experimental data.

The EPQFM approach is a microscopic one which takes care of LLL projection from the very beginning. However, the charge sector was explicitly projected out, the connection and coupling between the charge sector which displays Fractional Quantum Hall effect and the spin sector which displays interlayer phase coherence was not obvious in this approach. While in the CB theory, it is hard to incorporate the LLL projection (see however [24]), some parameters can only be taken as phenomenological parameters to be fitted into the microscopic LLL+HF calculations or experimental data. It is an effective low energy theory, special care is needed to capture some physics at microscopic length scales. The two approaches are complimentary to each other.

Consider a bi-layer system with N_1 (N_2) electrons in top (bottom) layer and with interlayer distance d in the presence of magnetic field $\vec{B} = \nabla \times \vec{A}$:

$$H = H_0 + H_{int}$$

$$H_0 = \int d^2x c_\alpha^\dagger(\vec{x}) \frac{(-i\hbar\vec{\nabla} + \frac{e}{c}\vec{A}(\vec{x}))^2}{2m} c_\alpha(\vec{x})$$

$$H_{int} = \frac{1}{2} \int d^2x d^2x' \delta\rho_\alpha(\vec{x}) V_{\alpha\beta}(\vec{x} - \vec{x}') \delta\rho_\beta(\vec{x}') \quad (1)$$

where electrons have *bare* mass m and carry charge $-e$, $c_\alpha, \alpha = 1, 2$ are electron operators in top and bottom layers, $\delta\rho_\alpha(\vec{x}) = c_\alpha^\dagger(\vec{x})c_\alpha(\vec{x}) - n_\alpha, \alpha = 1, 2$ are normal ordered electron densities on each layer. The intralayer interactions are $V_{11} = V_{22} = e^2/\epsilon r$, while interlayer interaction is $V_{12} = V_{21} = e^2/\epsilon\sqrt{r^2 + d^2}$ where ϵ is the dielectric constant. For imbalanced bi-layers, $n_1 \neq n_2$, but the background positive charges are still the same in the two layers, the chemical potential term is already included in H_{int} in Eqn.1.

The rest of the paper is organized as follows. In section II, we use a MCF theory to study the BLQH. We achieve some success, but also run into many troublesome problems. In section III, we use a CB theory which puts spin and charge sector on the same footing to study the BLQH. We demonstrate why this CB theory naturally avoid all the problems suffered in the MCF approach. We also compare the CB approach with the EPQFM approach and point out advantages and limitations of both approaches. Then we study the effects of imbalance on both ILCQH state and QDIS. In the final section, we summarized the main results of the paper and concluded that CB theory is superior to MCF approach in BLQH systems with broken symmetry.

II. MUTUAL COMPOSITE FERMION APPROACH: SUCCESS AND FAILURE

In parallel to advances in bi-layer QH systems, much progress has been made on novel physics involving quasi-particles and vortices in high temperature superconductors. Anderson employed a single-valued singular gauge transformation to study the quasi-particle energy spectrum in the vortex lattice state [16]. By employing the Anderson transformation, the author studied the quasi-particle transport in random vortex array in the mixed state [17]. Balents *et al*, investigated the zero temperature quantum phase transition from *d*-wave superconductor to underdoped side by assuming the transition is driven by the condensations of quantum fluctuation generated vortices [18,19]. The author extended the Anderson singular gauge transformation for static vortices to a mutual singular gauge transformation for quantum fluctuation generated dynamic vortices to study the novel interactions between quasi-particles and vortices near this quantum phase transition [19].

In this section, by employing essentially the same singular gauge transformation used to study the interactions between quasi-particles and vortices in high temperature superconductors, we revisit the bi-layer QH systems.

(1) Singular Gauge Transformation:

Performing a single-valued singular gauge transformation (SGT) [19,20]:

$$U = e^{i\tilde{\phi}} \int d^2x \int d^2x' \rho_1(\vec{x}) \arg(\vec{x} - \vec{x}') \rho_2(\vec{x}'), \quad \tilde{\phi} = 1 \quad (2)$$

we can transform the above Hamiltonian into:

$$H_0 = \int d^2x \psi_\alpha^\dagger(\vec{x}) \frac{(-i\hbar\vec{\nabla} + \frac{e}{c}\vec{A}(\vec{x}) - \hbar\vec{a}_\alpha(\vec{x}))^2}{2m} \psi_\alpha(\vec{x}) \quad (3)$$

where the transformed fermion is given by:

$$\begin{aligned} \psi_1(\vec{x}) &= U c_1(\vec{x}) U^{-1} = c_1(\vec{x}) e^{i \int d^2x' \arg(\vec{x} - \vec{x}') \rho_2(\vec{x}')} \\ \psi_2(\vec{x}) &= U c_2(\vec{x}) U^{-1} = c_2(\vec{x}) e^{i \int d^2x' \arg(\vec{x}' - \vec{x}) \rho_1(\vec{x}')} \end{aligned} \quad (4)$$

and the two mutual Chern-Simon (CS) gauge fields a_α satisfies: $\nabla \cdot \vec{a}_\alpha = 0$, $\nabla \times \vec{a}_\alpha = 2\pi\rho_{\bar{\alpha}}(\vec{x})$. Obviously, the interaction term is unaffected by the singular-gauge transformation. Note that it is $\arg(\vec{x} - \vec{x}')$ appearing in $\psi_1(\vec{x})$, while $\arg(\vec{x}' - \vec{x})$ appearing in $\psi_2(\vec{x})$ in Eqn.4. This subtle difference is crucial to prove all the commutation relations are kept intact by the single-valued singular gauge transformation Eqn.2. Note also that $\arg(\vec{x}' - \vec{x})$ works equally well in Eqn.2.

It is easy to check that in single layer system where $\rho_1 = \rho_2 = \rho$, Eqn.2 reduces to the conventional singular gauge transformation employed in [23]:

$$\psi_a(\vec{x}) = e^{i2 \int d^2x' \arg(\vec{x} - \vec{x}') \rho_a(\vec{x}')} c_a(\vec{x}) \quad (5)$$

where $\rho_a(\vec{x}) = c_a^\dagger(\vec{x}) c_a(\vec{x})$ is the electron density in layer $a = 1, 2$. It puts *two* flux quanta in the opposite direction to the external magnetic field at the position of each electron (Fig. 1 b). On the average, a CF feels a reduced effective field which is the external magnetic field minus the attached flux quanta.

For $\nu_T = 1$ bi-layer system, Eqn.4 puts *one* flux quantum in one layer in the opposite direction to the external magnetic field at the position directly above or below each electron (Fig.1 a).

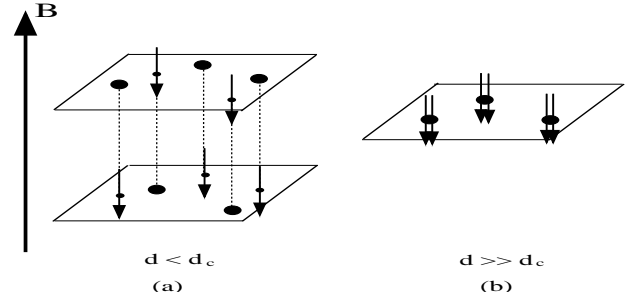


Fig 1: Contrast the flux attachment in Eqn.2 (a) with that in Eqn.5 (b). For simplicity, we only show three electrons in the top layer and two electrons in the bottom layer

On the average, a Mutual Composite Fermion (MCF) in each layer feels a reduced effective field which is the external magnetic field minus the inserted flux quanta in this layer. In single layer system, it is essential to attach even number of flux quanta to keep Fermi statistics intact. The two attached flux quanta are moving together with the associated electron. However, in bi-layer system, inserting one flux quantum does keep Fermi statistics intact. The inserted one flux quantum in one layer is moving together with its associated electron in the other layer. If choosing $\tilde{\phi}=1/2$, the transformation is not single-valued, the statistics is changed from fermion to boson, this choice will be pursued in the next section on Composite boson approach.

(2) Mean field theory:

In the following, we put $\hbar = c = e = \epsilon = 1$. At total filling factor $\nu_T = 1$, $\nabla \times \vec{A} = 2\pi n$ where $n = n_1 + n_2$ is the total average electron density. By absorbing the average values of C-S gauge fields $\nabla \times \langle \vec{a}_\alpha \rangle = 2\pi n_{\bar{\alpha}}$ into the external gauge potential $\vec{A}_\alpha^* = \vec{A} - \langle \vec{a}_\alpha \rangle$, we have:

$$H_0 = \int d^2x \psi_\alpha^\dagger(\vec{x}) \frac{(-i\vec{\nabla} + \vec{A}_\alpha^*(\vec{x}) - \delta\vec{a}_\alpha(\vec{x}))^2}{2m} \psi_\alpha(\vec{x}) \quad (6)$$

where $\nabla \times \vec{A}_\alpha^* = 2\pi n_\alpha$ and $\nabla \times \delta\vec{a}_\alpha = 2\pi\delta\rho_{\bar{\alpha}}(\vec{x})$ are the deviations from the corresponding average density (In the following, we will simply use a_α to stand for these deviations).

When $d < d_c$, the strong inter-layer interactions renormalize the bare mass into two effective masses m_α^* [24]. MCF in each layer feel effective magnetic field $B_\alpha^* =$

$\nabla \times \vec{A}_\alpha^* = 2\pi n_\alpha$, therefore fill exactly one MCF Landau level. The energy gaps are simply the cyclotron gaps of the MCF Landau levels $\omega_{c\alpha}^* = \frac{B_\alpha^*}{m_\alpha^*}$.

(3) *Fractional charges:*

Let's look at the charge of quasi-particles created by MCF field operators $\psi_\alpha^\dagger(\vec{x})$. Intuitively, inserting $\psi_1^\dagger(\vec{x})$ on layer 1 not only inserts an electron in layer 1 at position \vec{x} , but also pushes $\nu_2 = \frac{N_2}{N}$ electrons in layer 2 into its boundary, therefore induces a local charge deficit at \vec{x} in layer 2 which carries charge ν_2 , the total charge at \vec{x} is $e_1^* = -1 + \nu_2 = -\nu_1$. If \vec{x} and \vec{y} are two points far apart, then the product of operators $\psi_1^\dagger(\vec{x})\psi_1(\vec{y})$ in layer 1 will create a pair of fractional charges $\pm e_1^*$ at positions \vec{x} and \vec{y} with the charge gap $\hbar\omega_{c1}^*$. Similarly, inserting $\psi_2^\dagger(\vec{x})$ in layer 2 will create a charge $e_2^* = -1 + \nu_1 = -\nu_2$ at \vec{x} (note that $e_1^* + e_2^* = -1$). The product of operators $\psi_2^\dagger(\vec{x})\psi_2(\vec{y})$ in layer 2 will create a pair of fractional charges $\pm e_2^*$ at \vec{x} and \vec{y} with the charge gap $\hbar\omega_{c2}^*$. Only when the two layers are identical $N_1 = N_2$, $e_1^* = e_2^* = -1/2$ which carries fractional charge of even denominators. In general, the imbalanced bilayer system supports continuously changing total fractional charges in the thermodynamic limit.

The above arguments give the correct *total* fractional charges $\pm e_1^*, \pm e_2^*$. However, it can not determine the *relative* charge distributions between the two layers. At mean field level, the energies of all the possible relative charge differences are degenerate. The lowest energy configuration can only be determined by fluctuations. The above arguments are at most intuitive. The much more rigorous and elegant topological arguments can only be given in the composite boson theory of the next section.

(4) *Fluctuations:*

When considering fluctuations around the MCF mean field theory, it is convenient to go to Lagrangian [24]:

$$\begin{aligned} \mathcal{L} = & \psi_\alpha^\dagger(\partial_\tau - ia_0^\alpha)\psi_\alpha + \psi_\alpha^\dagger \frac{(-i\vec{\nabla} + \vec{A}^\alpha - \vec{a}^\alpha)^2}{2m_\alpha^*} \psi_\alpha \\ & + ia_0^\alpha n_\alpha + \frac{iq}{2\pi}(\sigma_1)_{\alpha\beta}a_0^\alpha a_t^\beta \\ & + \frac{q}{4\pi}(a_t^1 a_t^1 + a_t^2 a_t^2 + 2e^{-qd}a_t^1 a_t^2) \end{aligned} \quad (7)$$

where the constraints have been used to rewrite the Coulomb interactions and a_t^α is the transverse spatial component of gauge field in Coulomb gauge $\nabla \cdot \vec{a}_\alpha = 0$ [23,25] (In Lorenz invariant gauge the second to the last term becomes the mutual C-S term [19] $\frac{i}{4\pi}(\sigma_1)_{\alpha\beta}\epsilon_{\mu\nu\lambda}a_\mu^\alpha\partial_\nu a_\lambda^\beta$ where α, β refer to layer indices, while μ, ν, λ refer to space-time indices). The Hamiltonian has local $U(1)_1 \times U(1)_2$ gauge symmetry which corresponds to the invariance under $\psi_\alpha(\vec{x}) \rightarrow e^{i\theta_\alpha(\vec{x})}\psi_\alpha(\vec{x})$, $a_\mu^\alpha \rightarrow a_\mu^\alpha + \partial_\mu\theta_\alpha$.

Integrating out MCF ψ_1, ψ_2 to one-loop and carefully expanding the interlayer Coulomb interaction to the necessary order in the long-wavelength limit leads to:

$$\begin{aligned} \mathcal{L} = & \frac{iq}{2\pi}a_0^+ a_t^+ + \frac{q}{4\pi}(a_t^+)^2 \\ & + \frac{\epsilon_+}{4}q^2(a_0^+)^2 + \frac{1}{4}(\epsilon_+\omega^2 + (\chi_+ - \frac{d}{2\pi})q^2)(a_t^+)^2 \\ & + \frac{\epsilon_+}{4}q^2(a_0^-)^2 + \frac{1}{4}(\epsilon_+\omega^2 + (\chi_+ + \frac{d}{2\pi})q^2)(a_t^-)^2 \\ & + \frac{\epsilon_-}{2}q^2a_0^+ a_0^- + \frac{1}{2}(\epsilon_-\omega^2 + \chi_-q^2)a_t^+ a_t^- + \dots \end{aligned} \quad (8)$$

where \dots are higher gradient terms and a_t^α is the transverse component of gauge field in Coulomb gauge $\nabla \cdot \vec{a}_\alpha = 0$ [23,25], $a_\mu^\pm = a_\mu^1 \pm a_\mu^2$ and $\epsilon_\pm = \frac{1}{2}(\epsilon_1 \pm \epsilon_2)$, $\chi_\pm = \frac{1}{2}(\chi_1 \pm \chi_2)$. a^+ (a^-) stands for the total (relative) density fluctuation. a_μ^- is the NGM identified previously [6–8]. The dielectric constants $\epsilon_\alpha = \frac{m_\alpha^*}{2\pi B_\alpha}$ and the susceptibilities $\chi_\alpha = \frac{1}{2\pi m_\alpha^*}$ were calculated in single layer system in [22].

The first two terms are C-S term and Coulomb interaction term for + gauge field which take exactly the same forms as in a single layer system [23,25]. The third and the fourth terms are non-relativistic Maxwell terms for + and - modes respectively. The last two terms couple + mode to - mode. Integrating out + modes leads to $\epsilon_-^2 q^3(a_0^-)^2 + \epsilon_-(\epsilon_-\omega^2 + \chi_-q^2)(iq a_0^- a_t^-)$ which are sub-leading to the Maxwell term of a_0^-, a_t^- . In fact, these terms break Time reversal and Parity, in principle, a C-S term $iq a_0^- a_t^-$ will be generated under RG sense. However, the coefficient of this generated C-S term could be so small that it can be neglected except at experimentally unattainable low temperatures.

(5) *Neutral Gapless modes:*

For simplicity, we only consider the balanced case and will comment on im-balanced case later. Note that $\nabla \times \vec{a}^- = 2\pi\delta\rho$ where $\delta\rho = \delta\rho_2(\vec{x}) - \delta\rho_1(\vec{x})$ is the relative density fluctuation of the two layers. Introducing a variable ϕ which is conjugate to $\delta\rho(\vec{x})$, namely $[\phi(\vec{x}), \delta\rho(\vec{x}')] = i\delta(\vec{x} - \vec{x}')$, we can write a spin-wave Hamiltonian density:

$$\mathcal{H} = \frac{1}{2}\chi_s^{-1}(\delta\rho)^2 + \frac{1}{2}\rho_s(\nabla\phi)^2 \quad (9)$$

If $\delta\rho$ is treated as a continuous variable, then ϕ is a free field varying from $-\infty$ to ∞ . By integrating out $\delta\rho$, we get the ϕ representation:

$$\mathcal{L}_\phi = \frac{1}{2}\chi_s(\partial_\tau\phi)^2 + \frac{1}{2}\rho_s(\nabla\phi)^2 \quad (10)$$

Integrating out ϕ , we get an effective action density in the $\delta\rho$ representation which is dual to the above ϕ representation:

$$\mathcal{L}_\rho = \frac{1}{2}\chi_s^{-1}(\delta\rho)^2 + \frac{1}{2}\rho_s^{-1}(\frac{\omega}{q})^2(\delta\rho)^2 \quad (11)$$

Plugging the constraint $\nabla \times \vec{a}^- = 2\pi\delta\rho$ into Eqn.11, we get:

$$\mathcal{L}_a = \frac{1}{2}(\rho_s^{-1}\omega^2 + \chi_s^{-1}q^2)(a_t^-)^2 \quad (12)$$

This is consistent with the well-known fact that a *pure* $2+1$ dimensional $U(1)$ gauge field is dual to a $2+1$ dimensional Gaussian model which does not have any topological excitations [26]. Comparing Eqn.12 with Eqn.8 (for simplicity, we take $N_1 = N_2$), we get $\rho_s = \hbar\omega_c^*/\pi, \chi_s = [2\pi^2(\chi + \frac{d}{2\pi})]^{-1}$. So the spin stiffness scales as the cyclotron gap and the finite charge gap of MCF implies finite spin stiffness. In order to compare with experimental data in [4,5], we have to put back \hbar, c, e, ϵ and find the spin-wave velocity:

$$v^2 = \rho_s/\chi_s = \frac{(\omega_c^*)^2}{\pi n} + \left(\frac{\alpha c}{\epsilon}\right)\left(\frac{d}{l}\right)\frac{\omega_c^*}{\sqrt{2\pi n}} \quad (13)$$

where n is the total density, l is the magnetic length and $\alpha \sim 1/137$ is the fine structure constant. Note that the correct expansion of interlayer Coulomb interaction is crucial to get the second term.

By measuring the transport properties at finite temperature, the authors in [5] found the activation gap $E_A \sim 0.4K$. By setting $E_A = \hbar\omega_c^*$ and plugging the experimental parameters $n = 5.2 \times 10^{10} \text{ cm}^{-2}, d/l = 1.61, \epsilon = 12.6$ into Eqn.13, we find that the first term is $1.65 \times 10^{10} (\text{cm/s})^2$, the second term is $2.54 \times 10^{12} (\text{cm/s})^2$ which is two orders of magnitude bigger than the first term. Finally, we find $v \sim 1.59 \times 10^6 \text{ cm/s}$ which is dominated by the second term. This value is in good agreement with $v \sim 1.4 \times 10^6 \text{ cm/s}$ found in [4].

(6) Topological excitations:

As discussed in the previous paragraph, at mean field theory, there are four kinds of gapped excitations with total fractional charges $\pm e_1^* = \pm \nu_1$ and $\pm e_2^* = \pm \nu_2$ which, for example, can be excited by finite temperature close to $\hbar\omega_c^*$. But their relative charge distributions between the two layers are undetermined. In fact, all the possible excitations can be characterized by their (a^+, a^-) charges (q_+, q_-) . For example, the four kinds of excitations are denoted by $(\pm \nu_1, q_-), (\pm \nu_2, q_-)$. For $\nu_1 = \nu_2$, they reduce to two sets: $(\pm \frac{1}{2}, q_-)$. If $\delta\rho$ in Eqn.9 is treated as a discrete variable, then $0 < \phi < 2\pi$ is an angle variable. q_- must be integers $0, \pm 1, \dots$. Exchanging a^+ leads to $1/r$ interaction between the four sets of beasts. While exchanging a^- leads to logarithmic interactions which lead to a bound state between two beasts with opposite $q_- \neq 0$. The energy of this bound state with length L is $E_b = \Delta_+ + \Delta_- + q_+^2 \frac{e^2}{L} + q_-^2 \hbar\omega_c^* \ln L/l$ where Δ_+ and Δ_- are the core energies of QH and QP respectively.

An important question to ask is what is the gluing conditions (or selection rules) of (q_+, q_-) for the realizable excitations ? Namely, what is spin (q_-) and charge (q_+) connection ? Two specific questions are: (1) Is there a charge neutral vortex excitation with $(0, \pm 1)$? Being charge neutral, this kind of excitation is a bosonic excitation. (2) Is there a charge $\pm 1/2$ and spin neutral excitation $(\pm 1/2, 0)$? If they do exist, then the

QP and QH pair with $q_- = 0$ have the lowest energy $\hbar\omega_c^* = \Delta_+ + \Delta_-$. They decouple from a^- gauge field, therefore interact with each other only with $1/r$ interaction and are asymptotically free even at $T = 0$ just like those in single layer system. Their charges are evenly distributed in the two layers (namely carry fractional charges $\pm 1/4$ in each separate layer). They are deconfined $\pm 1/2$ excitations which are completely different excitations from merons which are confined logarithmically.

Unfortunately, the spin-charge connection is far from obvious in this MCF approach. So little can be said about these two possibilities. In the composite boson approach to be presented in the next section, both interesting possibilities are ruled out.

(7) Extension to other filling factors:

Let's briefly discuss $\nu_T = 1/2$ bilayer system. It is well known that this state is described by Halperin's 331 state [1]. In this state, the singular gauge transformation $U = e^{i \int d^2x \int d^2x' U_{\alpha\beta} \rho_\alpha(\vec{x}) \text{arg}(\vec{x} - \vec{x}') \rho_\beta(\vec{x}')}$ where the matrix $U = \frac{1}{2} \begin{pmatrix} 2 & 1 \\ 1 & 2 \end{pmatrix}$ attached two intralayer flux quanta and one interlayer flux quantum to electrons to form Entangled Composite Fermions (ECF). At layer 1 (layer 2), the filling factor of ECF is $\nu_1^* = \frac{N_1}{N_2}$ ($\nu_2^* = \frac{N_2}{N_1}$). Only when the two layers are identical $N_1 = N_2$, we get $\nu_1^* = \nu_2^* = 1$ QH states on both layers, therefore $\nu_T = 1/2$ system lacks interlayer coherence.

(8) Comparison with another version of CF approach:

It is instructive to compare our MCF picture developed in this section with the earlier pictures proposed in [13,14]. When $N_1 = N_2$, the authors in [13] attached $\tilde{\phi} = 2$ flux quanta of layer 2 to electrons in layer 1 or vice versa to form interlayer composite fermions so that at mean field theory, CF in each layer form a compressible Fermi liquid. They conjectured that a^- gauge field fluctuation mediates an attractive interaction between CF in different layers which leads to a (likely p-wave) pairing instability. This pairing between CF in different layers opens an energy gap. But no systematic theory is developed along this picture. In the MCF picture studied in this section, there is a *charge* gap which is equal to the cyclotron gap even at mean field theory which is robust against any gauge field fluctuation. Due to using $\tilde{\phi} = 2$, the authors in [14] concluded that the mutual Hall drag resistivity is $2h/e^2$ which is inconsistent with the experimental result in [5].

(9) Interlayer tunneling:

The interlayer tunneling term is:

$$H_t = tc_1^\dagger(\vec{x})c_2(\vec{x}) + h.c. \quad (14)$$

Substituting Eqn.4 into above equation leads to:

$$H_t = t\psi_1^\dagger(\vec{x})e^{i \int d^2x' [\text{arg}(\vec{x} - \vec{x}')\rho_2(\vec{x}') - \text{arg}(\vec{x}' - \vec{x})\rho_1(\vec{x}')]}\psi_2(\vec{x}') + h.c. \quad (15)$$

This is a very awkward equation to deal with.

The authors in [7] pointed out that the tunneling process of an electron from one layer to the other corresponds to an instanton in the $2 + 1$ dimensional compact QED. They applied the results of Polyakov on instanton- anti-instanton plasma on $2 + 1$ dimensional compact QED and found the effective action:

$$\mathcal{L} = \frac{1}{g^2}(\partial_\mu \chi)^2 + \frac{t}{2\pi l^2} \cos \chi \quad (16)$$

where g is the $U(1)$ gauge coupling constant given in Eqn.10. In the original work of Polyakov, χ is a non-compact field $-\infty < \chi < \infty$. The compactness of χ was forced in an ad hoc way in [7]. Note that the compactness of QED has nothing to do with the compactness of χ .

(10) *Summary of limited success of MCF theory:*

We use a Mutual Composite Fermion (MCF) picture to explain the interlayer coherent incompressible phase at $d < d_c$. This MCF is a generalization of Composite Fermion (CF) in single layer QH systems to bilayer QH systems [21,23,22,24]. In the mean field picture, MCF in each layer fill exactly $\nu^* = 1$ MCF Landau level. There are four kinds of gapped quasi-particles (QP) and quasi-holes (QH) with total fractional charges $\pm e_1^* = \pm \nu_1, \pm e_2^* = \pm \nu_2$ (For $\nu_1 = \nu_2 = 1/2$, they reduce to two sets). When considering the fluctuations above the $\nu^* = 1$ MCF QH states, we identify the NGM with linear dispersion relation $\omega \sim v k$ and determine v in terms of experimental measurable quantities. When interpreting the activation gap E_A found in [5] in terms of the cyclotron gap of the $\nu^* = 1$ MCF Landau level, we calculate v and find its value is in good agreement with the value determined in [4]. Tentatively, we intend to classify all the possible excitations in terms of a^+ and a^- charges (q_+, q_-).

(11) *Serious problems with MCF approach:*

Despite the success of the MCF approach mentioned above, there are many serious drawbacks of this approach. We list some of them in the following.

(a) The determination of the fractional charges is at most intuitive. A convincing determination can only be firmly established from the CB approach to be discussed in the next section. Furthermore, the MCF still carries charge 1, while the QP or QH carry charge $\pm 1/2$. An extension of Murthy-Shankar formalism [24] in SLQH to BLQH may be needed to express physics in terms of these $\pm 1/2$ QP and QH.

(b) It is easy to see that the spin wave dispersion in Eqn.13 remains linear $\omega \sim v k$ even in the $d \rightarrow 0$ limit. This contradicts with the well established fact that in the $d \rightarrow 0$ limit, the linear dispersion relation will be replaced by quadratic Ferromagnetic spin-wave dispersion relation $\omega \sim k^2$ due to the enlarged $SU(2)$ symmetry at $d \rightarrow 0$. This is because the flux attachment singular

gauge transformation Eqn.2 breaks $SU(2)$ symmetry at very beginning even in the $d \rightarrow 0$ limit.

(c) The broken symmetry in the ground state is not obvious without resorting to the (111) wavefunction. The origin of the gapless mode is not clear.

(d) The compactness of the angle ϕ in Eqn.10 was put in by hand in an ad hoc way.

(e) The spin-charge connection in (q_+, q_-) can not be determined.

(f) The tunneling term can not be derived in a straightforward way.

(g) In the imbalanced case, there are two MCF cyclotron gaps $\hbar\omega_{c\alpha}^*$ at mean field theory. However, there is only one charge gap in the system. It is not known how to reconcile this discrepancy within MCF approach.

(h) It is not known how to push the MCF theory further to study the quantum disordered side.

In the following, we will show that the alternative CB approach not only can achieve all the results in this section, but also can get rid of all these drawbacks naturally.

III. COMPOSITE BOSON APPROACH

Composite boson approach originated from Girvin and Macdonald's off-diagonal long range order [27], formulated in terms of Chern-Simon Ginsburg- Landau theory [28]. It has been successfully applied to Laughlin's series $\nu = \frac{1}{2s+1}$ [28] and $\nu = 1$ spin unpolarized QH system [29]. It has also been applied to BLQH [8,10]. Unfortunately, it may not be applied to study Jain's series at $\nu = \frac{p}{2sp \pm 1}$ with $p \neq 1$ and $\nu = 1/2$ Fermi Liquid system. In this section, we applied CSGL theory to study imbalanced bi-layer QH system. Instead of integrating out the charge degree of freedoms which was done in all the previous CB approach [8,9], we keep charge and spin degree of freedoms on the same footing and explicitly stress the spin and charge connection. We study how the imbalance affects various physical quantities such as spin wave velocity, the meron pair distance and energy, the critical in-plane field for commensurate-incommensurate transition, etc. We also study the quantum phase transition from interlayer in-coherent state to interlayer coherent state driven by the boson condensation induced by the imbalance.

We can rewrite H_{int} in Eqn.1 as:

$$\begin{aligned} H_{int} &= \frac{1}{2}\delta\rho_1 V \delta\rho_1 + \frac{1}{2}\delta\rho_2 V \delta\rho_2 + \delta\rho_1 \tilde{V} \delta\rho_2 \\ &= \frac{1}{2}\delta\rho_+ V_+ \delta\rho_+ + \frac{1}{2}\delta\rho_- V_- \delta\rho_- \end{aligned} \quad (17)$$

where $V = V_{11} = V_{22}, \tilde{V} = V_{12}, V_+ = \frac{V+\tilde{V}}{2}, V_- = \frac{V-\tilde{V}}{2}$ and $\delta\rho_\pm = \delta\rho_1 \pm \delta\rho_2$.

Performing a singular gauge transformation [19,20]:

$$\phi_a(\vec{x}) = e^{i \int d^2x' \arg(\vec{x}-\vec{x}') \rho(\vec{x}')} c_a(\vec{x}) \quad (18)$$

where $\rho(\vec{x}) = c_1^\dagger(\vec{x})c_1(\vec{x}) + c_2^\dagger(\vec{x})c_2(\vec{x})$ is the total density of the bi-layer system. Note that this transformation treats both c_1 and c_2 on the same footing. This is reasonable only when the distance between the two layers is sufficiently small.

It can be shown that $\phi_a(\vec{x})$ satisfies all the boson commutation relations. It can be shown that this SGT is the same as that in Eqn.2 if we choose $\tilde{\phi} = 1/2$ and replace both ρ_1 and ρ_2 by $\rho = \rho_1 + \rho_2$. Because the SGT with $\tilde{\phi} = 1/2$ in Eqn.2 is not single-valued, the statistics is changed from fermion to boson.

We can transform the Hamiltonian Eqn.1 into the Lagrangian in Coulomb gauge:

$$\begin{aligned} \mathcal{L} = & \phi_a^\dagger(\partial_\tau - ia_0)\phi_a + \phi_a^\dagger(\vec{x}) \frac{(-i\hbar\vec{\nabla} + \frac{e}{c}\vec{A}(\vec{x}) - \hbar\vec{a}(\vec{x}))^2}{2m} \phi_a(\vec{x}) \\ & + \frac{1}{2} \int d^2x' \delta\rho(\vec{x}) V_+(\vec{x} - \vec{x}') \delta\rho(\vec{x}') \\ & + \frac{1}{2} \int d^2x' \delta\rho_-(\vec{x}) V_-(\vec{x} - \vec{x}') \delta\rho_-(\vec{x}') - \frac{i}{2\pi} a_0(\nabla \times \vec{a}) \end{aligned} \quad (19)$$

In Coulomb gauge, integrating out a_0 leads to the constraint: $\nabla \times \vec{a} = 2\pi\phi_a^\dagger\phi_a$.

By taking full advantage of the easy-plane anisotropy shown in Eqn.19, we can write the two bosons in terms of magnitude and phase

$$\phi_a = \sqrt{\bar{\rho}_a + \delta\rho_a} e^{i\theta_a} \quad (20)$$

The boson commutation relations imply that $[\delta\rho_a(\vec{x}), \phi_b(\vec{x})] = i\hbar\delta_{ab}\delta(\vec{x} - \vec{x}')$.

We can see Eqn.19 has a local $U(1)$ gauge symmetry $\theta_a \rightarrow \theta_a + \chi$, $a_\mu \rightarrow a_\mu + \partial_\mu\chi$ and also a global $U(1)$ symmetry $\theta_1 \rightarrow \theta_1 + \chi$, $\theta_2 \rightarrow \theta_2 - \chi$. We denote the symmetry by $U(1)_L \times U(1)_G$.

Absorbing the external gauge potential \vec{A} into \vec{a} and substituting Eqn.20 into Eqn.19, we get:

$$\begin{aligned} \mathcal{L} = & \frac{1}{2}\partial_\tau\delta\rho^+ + \frac{1}{2}\bar{\rho}_+i\partial_\tau\theta_+ + \frac{i}{2}\delta\rho^+(\partial_\tau\theta^+ - 2a_0) \\ & + \frac{\bar{\rho}_a + \delta\rho_a}{2m}(\nabla\theta_a - \vec{a})^2 + \frac{1}{2}\delta\rho^+V_+(\vec{q})\delta\rho^+ - \frac{i}{2\pi}a_0(\nabla \times \vec{a}) \\ & + \frac{i}{2}(\delta\rho^- + \bar{\rho}_-)\partial_\tau\theta^- + \frac{1}{2}\delta\rho^-V_-(\vec{q})\delta\rho^- \end{aligned} \quad (21)$$

where $\delta\rho^\pm = \delta\rho_1 \pm \delta\rho_2$, $\theta_\pm = \theta_1 \pm \theta_2$. They satisfy the commutation relations $[\delta\rho_\alpha(\vec{x}), \theta_\beta(\vec{x}')] = 2i\hbar\delta_{\alpha\beta}\delta(\vec{x} - \vec{x}')$ where $\alpha, \beta = \pm$.

It is easy to see that the symmetry is $U(1)_+ \times U(1)_-$ where $U(1)_+$ is a local gauge symmetry, while $U(1)_-$ is a global symmetry. We also note that it is $\delta\rho^- + \bar{\rho}_- = (\delta\rho_1 - \delta\rho_2) + (\bar{\rho}_1 - \bar{\rho}_2) = \rho_1 - \rho_2$ which is conjugate to the phase θ_- , namely, $[\delta\rho^-(\vec{x}) + \bar{\rho}_-, \theta_-(\vec{x}')] = 2i\hbar\delta(\vec{x} - \vec{x}')$. In the following, for the simplicity of notation, we redefine $\delta\rho^- = \rho_1 - \rho_2$, then the last two terms in Eqn.21 becomes:

$$\frac{i}{2}\delta\rho^-\partial_\tau\theta^- + \frac{1}{2}\delta\rho^-V_-(\vec{q})\delta\rho^- - h_z\delta\rho^- \quad (22)$$

where $h_z = V_- \bar{\rho}_- = V_-(\bar{\rho}_1 - \bar{\rho}_2)$ plays a role like a Zeeman field.

By expressing the spatial gradient term in Eqn.21 in terms of $(\delta\rho_+, \theta_+)$ and $(\delta\rho_-, \theta_-)$, we find

$$\begin{aligned} \mathcal{L} = & i\delta\rho^+(\frac{1}{2}\partial_\tau\theta^+ - a_0) + \frac{\bar{\rho}}{2m}[\frac{1}{2}\nabla\theta_+ + \frac{1}{2}(\nu_1 - \nu_2)\nabla\theta_- - \vec{a}]^2 \\ & + \frac{1}{2}\delta\rho^+V_+(\vec{q})\delta\rho^+ - \frac{i}{2\pi}a_0(\nabla \times \vec{a}) \\ & + \frac{i}{2}\delta\rho^-\partial_\tau\theta^- + \frac{\bar{\rho}f}{2m}(\frac{1}{2}\nabla\theta_-)^2 + \frac{1}{2}\delta\rho^-V_-(\vec{q})\delta\rho^- - h_z\delta\rho^- \end{aligned} \quad (23)$$

where $f = 4\nu_1\nu_2$ which is equal to 1 at the balanced case.

Plus the extra terms due to the magnitude fluctuations in the spatial gradient terms:

$$\begin{aligned} \frac{\delta\rho_a}{2m}(\nabla\theta_a - \vec{a})^2 = & \frac{\delta\rho^+}{2m}[(\frac{1}{2}\nabla\theta_+ - \vec{a})^2 + (\frac{1}{2}\nabla\theta_-)^2] \\ & + \frac{\delta\rho^-}{2m}(\frac{1}{2}\nabla\theta_+ - \vec{a}) \cdot \nabla\theta_- \end{aligned} \quad (24)$$

Note that in Eqn.24 both $\delta\rho^+$ and $\delta\rho^-$ couple to terms with two spatial gradients, therefore can be dropped relative to the terms in Eqn.23 which contains just one temporal gradient.

In the following, we will discuss balanced and imbalanced cases separately:

A. Balanced case $\nu_1 = \nu_2 = 1/2$

Putting $\nu_1 = \nu_2 = 1/2$ and $h_z = 0$ into Eqn.23, we get the Lagrangian in the balanced case:

$$\begin{aligned} \mathcal{L} = & i\delta\rho^+(\frac{1}{2}\partial_\tau\theta^+ - a_0) + \frac{\bar{\rho}}{2m}(\frac{1}{2}\nabla\theta_+ - \vec{a})^2 \\ & + \frac{1}{2}\delta\rho^+V_+(\vec{q})\delta\rho^+ - \frac{i}{2\pi}a_0(\nabla \times \vec{a}) \\ & + \frac{i}{2}\delta\rho^-\partial_\tau\theta^- + \frac{\bar{\rho}}{2m}(\frac{1}{2}\nabla\theta_-)^2 + \frac{1}{2}\delta\rho^-V_-(\vec{q})\delta\rho^- \end{aligned} \quad (25)$$

In the balanced case, the symmetry is enlarged to $U(1)_L \times U(1)_G \times Z_2$ where the global Z_2 symmetry is the exchange symmetry between layer 1 and layer 2. At temperatures much lower than the vortex excitation energy, we can neglect vortex configurations in Eqn.25 and only consider the low energy spin-wave excitation. The charge sector (θ^+ mode) and spin sector (θ^- mode) are essentially decoupled.

(1) Off-diagonal algebraic order in the charge sector:

The charge sector is essentially the same as the CSGL action in BLQH. Using the constraint $a_t = \frac{2\pi\delta\rho^+}{q}$, neglecting vortex excitations in the ground state and integrating out $\delta\rho^+$ leads to the effective action of θ_+ :

$$\mathcal{L}_c = \frac{1}{8} \theta_+(-\vec{q}, -\omega) \left[\frac{\omega^2 + \omega_{\vec{q}}^2}{V_+(q) + \frac{4\pi^2 \bar{\rho}}{m} \frac{1}{q^2}} \right] \theta_+(\vec{q}, \omega) \quad (26)$$

where $\omega_{\vec{q}}^2 = \omega_c^2 + \frac{\bar{\rho}}{m} q^2 V_+(q)$ and $\omega_c = \frac{2\pi\bar{\rho}}{m}$ is the cyclotron frequency.

From Eqn.26, we can find the equal time correlator of θ_+ :

$$\begin{aligned} \langle \theta_+(-\vec{q}) \theta_+(\vec{q}) \rangle &= \int_{-\infty}^{\infty} \frac{d\omega}{2\pi} \langle \theta_+(-\vec{q}, -\omega) \theta_+(\vec{q}, \omega) \rangle \\ &= 2 \times \frac{2\pi}{q^2} + O\left(\frac{1}{q}\right) \end{aligned} \quad (27)$$

which leads to the algebraic order:

$$\langle e^{i(\theta_+(\vec{x}) - \theta_+(\vec{y}))} \rangle = \frac{1}{|x - y|^2} \quad (28)$$

Note that if we define $\tilde{\theta}_+ = \frac{\theta_1 + \theta_2}{2} = \theta_+/2$, then $\langle e^{i(\tilde{\theta}_+(\vec{x}) - \tilde{\theta}_+(\vec{y}))} \rangle = \frac{1}{|x - y|^{1/2}}$ which takes exactly the same form as that in $\nu = 1$ SLQH. However, when considering vortex excitations to be discussed in the following $e^{i\tilde{\theta}_+(\vec{x})}$ may not be single valued, therefore the fundamental angle variable is θ_+ instead of $\tilde{\theta}_+$.

(2) Spin-wave excitation:

While the spin sector has a neutral gapless mode. Integrating out $\delta\rho^-$ leads to

$$\mathcal{L}_s = \frac{1}{2V_-(\vec{q})} \left(\frac{1}{2} \partial_{\tau} \theta^- \right)^2 + \frac{\bar{\rho}}{2m} \left(\frac{1}{2} \nabla \theta_- \right)^2 \quad (29)$$

where the dispersion relation of spin wave can be extracted:

$$\omega^2 = \left[\frac{\bar{\rho}}{m} V_-(\vec{q}) \right] q^2 = v^2 q^2 \quad (30)$$

In the long wave-length limit:

$$V_-(\vec{q}) = \frac{\pi e^2}{\epsilon} \left(d - \frac{1}{2} d^2 q + \frac{1}{6} d^3 q^2 + \dots \right), \quad qd \ll 1 \quad (31)$$

The spin wave velocity is:

$$v^2 = \frac{\bar{\rho}}{m} \frac{\pi e^2}{\epsilon} d = \frac{e^2}{m\epsilon} \sqrt{\frac{\pi\bar{\rho}}{2}} \frac{d}{l} \quad (32)$$

Eqn.32 shows that the spin wave velocity should increase as \sqrt{d} when $d < d_c$. At $d = 0$, $v = 0$. This is expected, because at $d = 0$ the $U(1)_G$ symmetry is enlarged to $SU(2)_G$, the spin wave of isotropic ferromagnet $\omega \sim k^2$. By plugging the experimental parameters $m \sim 0.07m_e$ which is the band mass of *GaAs*, $\bar{\rho} = 5.2 \times 10^{10} \text{ cm}^{-2}$, $d/l = 1.61$, $\epsilon = 12.6$ into Eqn.32, we find that $v \sim 1.14 \times 10^7 \text{ cm/s}$. This value is about 8 times larger than the experimental value. Although Quantum fluctuations will renormalize down the spin stiffness from $\rho_{\text{bare}} = \bar{\rho}$ to $\rho_{\text{eff}} < \bar{\rho}$, it is known that CSGL theory can not give precise numerical values on energy gaps even in

SLQH. In fact, the spin stiffness ρ_s which is defined as $\frac{\rho_s}{2} (\nabla \theta_-)^2$ in Eqn.29 should be determined by the interlayer Coulomb interaction instead of being dependent of the band mass m .

It is constructive to compare the spin (-) sector of Eqn.25 with the EPQHF Hamiltonian achieved by the microscopic LLL+HF approach in [10]:

$$\begin{aligned} \mathcal{L} = & i \frac{\rho}{2} \vec{A}(\vec{m}) \cdot \partial_{\tau} \vec{m} + \beta_m (m_z)^2 - C q m_z (-\vec{q}) m_z (\vec{q}) \\ & + \frac{\rho_A}{2} (\nabla m_z)^2 + \frac{\rho_E}{2} [(\nabla m_x)^2 + (\nabla m_y)^2] \end{aligned} \quad (33)$$

where $\nabla \vec{m} \times \vec{A} = \vec{m}$, $\beta_m \sim d^2$, $C = \frac{e^2 d^2}{16\pi\epsilon}$, $\rho_A = \frac{e^2}{16\pi\epsilon l} \int_0^\infty dx x^2 \exp(-x^2/2) = \frac{e^2}{16\sqrt{2\pi}\epsilon l}$ is determined by the intralayer interaction and $\rho_E = \frac{e^2}{16\pi\epsilon l} \int_0^\infty dx x^2 \exp(-x^2/2 - dx/l)$ is determined by the interlayer interaction.

In the above equation, the first term is the Berry phase term, the second term is the mass (or capacitance) term, this term leads to the easy-plane anisotropy which suppresses the relative density fluctuations between the two layers, the third term is nonanalytic in the wave vector due to the long range nature of the Coulomb interaction, the fourth term is the spin stiffness term for m_z and the fifth term is the spin stiffness term for easy-plane. At $d = 0$, $\beta_m = C = 0$, $\rho_A = \rho_E = \frac{e^2}{16\sqrt{2\pi}\epsilon l}$, then \mathcal{L} in Eqn.33 reduces to the $SU(2)$ symmetric QH ferromagnet [29] as it should be. Note that the value of $\rho_A = \rho_E$ at $d = 0$ is exact, because the ground state wavefunction is exactly the Halperin (111) wavefunction, while at any finite d , the estimates of $\rho_A \neq \rho_E$ by HF approximation may be crude, because we still do not know what is the exact groundstate wavefunction which may be qualitatively different from the (111) wavefunction [10,30]. In the presence of the easy-plane (β_m) term, C and ρ_A terms are subleading, therefore, can be dropped.

If taking the symmetry breaking direction to be along the \hat{x} direction, we can write $m_x = \sqrt{1 - m_z^2} \cos \theta$, $m_y = \sqrt{1 - m_z^2} \sin \theta$, m_z with $m_z \sim 0$, $\theta \sim 0$. Substituting the parameterization into the Berry phase term in Eqn.33, we find the Berry phase term to be $i \frac{\bar{\rho}}{4} n_z \partial_{\tau} \theta$, if identifying $m_z = 2\delta\rho_-$, it is the same as the linear derivative ($\frac{i}{2} \delta\rho_- \partial_{\tau} \theta^-$) term in the spin sector of Eqn.25. However, we can see the leading term in Eqn.31 which leads to the capacitive term is $\sim d$, but in Eqn.33, it is $\sim d^2$, while the Monte-Carlo simulation in spherical geometry in [30] indicates it is $\sim d$. The subleading term in Eqn.31 is non-analytic $\sim q$ instead of $\sim q^2$, this is due to the long-range behavior of the Coulomb interaction. This non-analytic term is the same as that in Eqn.33 if identifying $m_z = 2\delta\rho_-$. The third term in Eqn.31 leads to a $(\nabla m_z)^2$ term with a coefficient $\sim d^3$, while the coefficient of $(\nabla m_z)^2$ term in Eqn.31 is ρ_A which approaches the constant $\frac{e^2}{16\sqrt{2\pi}\epsilon l}$ as $d \rightarrow 0$ as dictated by $SU(2)$ symmetry at $d = 0$. The difficulty to recover $SU(2)$ sym-

metric limit at $d = 0$ from the CB approach is due to that the decomposition Eqn.20 in our CB approach takes advantage of the easy-plane anisotropy from the very beginning. This is similar to Abelian bosonization versus Non-Abelian bosonization in one dimensional Luttinger liquid or multi-channel Kondo model [31].

By this detailed comparison between the CB approach and the microscopic LLL+HF approach, we find that the two approaches lead to exactly the same functional form in the spin sector, some coefficients such as the Berry phase term and the non-analytic term are the same, while some other coefficients such as the easy-plane term and spin stiffness term are not. Unfortunately, it is very difficult to incorporate the LLL projection in the CB approach. As suggested in [10], we should simply take some coefficients in CB approach as phenomenological values to be fitted into microscopic LLL+HF calculations or numerical calculations or eventually experimental data. The advantage of CB approach is that it also keeps the charge + sector explicitly, therefore treat the QH effects in the charge sector and the inter-layer phase coherence in the spin sector at the same footing. While the charge sector in the LLL+HF approach is completely integrated out.

(3) Topological excitations:

Any topological excitations are characterized by two winding numbers $\Delta\theta_1 = 2\pi m_1$, $\Delta\theta_2 = 2\pi m_2$, or equivalently, $\Delta\theta_+ = 2\pi(m_1 + m_2) = 2\pi m_+$, $\Delta\theta_- = 2\pi(m_1 - m_2) = 2\pi m_-$. It is important to realize that the two fundamental angles are θ_1, θ_2 instead of θ_+, θ_- . m_1, m_2 are two independent integers, while m_+, m_- are not, because $m_+ - m_- = 2m_2$ which has to be an even integer.

There are following 4 kinds of topological excitations: $\Delta\theta_1 = \pm 2\pi$, $\Delta\theta_2 = 0$ or $\Delta\theta_1 = 0$, $\Delta\theta_2 = \pm 2\pi$. Namely $(m_1, m_2) = (\pm 1, 0)$ or $(m_1, m_2) = (0, \pm 1)$. They correspond to inserting one flux quantum in layer 1 or 2, in the same or opposite direction as the external magnetic field. Let's classify all the topological excitations in terms of (q, m_-) where charge q is the fractional charge of the topological excitations in the following table.

	$(1, 0)$	$(-1, 0)$	$(0, 1)$	$(0, -1)$
m_-	1	-1	-1	1
m_+	1	-1	1	-1
q	$1/2$	$-1/2$	$1/2$	$-1/2$

Table 1: The fractional charge in the balanced case

The fractional charges in Table 1 were determined from the constraint $\nabla \times \vec{a} = 2\pi\delta\rho$ and the finiteness of the energy in the charge sector:

$$q = \frac{1}{2\pi} \oint \vec{a} \cdot d\vec{l} = \frac{1}{2\pi} \times \frac{1}{2} \oint \nabla\theta^+ \cdot d\vec{l} = \frac{1}{2}m_+ \quad (34)$$

$m_- = \pm 1$ gives the vorticities which lead to logarithmic interaction between the merons, while $q = \pm 1/2$ lead to $1/r$ interaction. Therefore merons are confined

into the following two possible pairs at low temperature. (1) Charge neutral pairs: $(\pm 1/2, \pm 1)$ or $(\pm 1/2, \mp 1)$. The NGM will turn into charge neutral pairs at large wavevectors (or short distance). The pair behaves as a boson. (2) Charge 1 pair $(1/2, \pm 1)$ or charge -1 pair $(-1/2, \pm 1)$. The pair behaves as a fermion. They are the lowest charged excitations in BLQH and the main dissipation sources for the charge transports. A duality transformation (See Eqn.42) can be easily performed to express low energy physics in terms of the dynamics of these topological excitations. There is a possible Kosterlitz-Thouless (KT) transition above which the meron pairs are liberated into free meron.

The MCF picture in the last section points to two interesting possibilities (1) There maybe Charge neutral bosonic excitations with $(0, \pm 1)$: Note that $m_+ = 0$ implies $m_1 = -m_2 = m$ and $m_- = 2m$. For $m = 1$, it corresponds to inserting one flux quantum in layer 1 in one direction and one flux quantum in layer 2 in the opposite direction. So only $(0, \pm 2)$ exist, while $(0, \pm 1)$ do not exist. (2) There may be deconfined (or free) $1/2$ charged excitations. Because any excitations with non-vanishing m_- will be confined, so any deconfined excitations must have $m_- = 0$ which implies $m_1 = m_2 = m$ and $m_+ = 2m$. We find the charge $q = \frac{1}{2}m_+ = m$ must be an integer. This proof rigorously rules out the possibility of the existence of deconfined fractional charges. We conclude that *any deconfined charge must be an integral charge*. $m = 1$ corresponds to inserting one flux quantum through both layers which is conventional charge 1 excitation. Splitting the two fluxes will turn into a a meron pair with the same charge.

Most of the results achieved in this subsection were achieved before [9,10,2] in microscopic calculations. In these calculations, the charge fluctuations were integrated out, the LLL projections were explicitly performed and HF approximations were made. Here, we reproduce these old results in a very simple way which keeps both spin and charge in the same footing and bring out the spin-charge connection in a very transparent way. We also classify all the possible excitations in this effective CB approach. In the next subsection, we will study the effects of the imbalance.

B. Im-balanced case $\nu_1 \neq \nu_2$

(1) Off-diagonal algebraic order and Spin-wave excitation:

In the im-balanced case, the second term in Eqn.23 includes the coupling between spin sector and charge sector even when neglecting vortex excitations. Expanding this term, we find the effective action of the coupled θ_+ and θ_- modes:

$$\begin{aligned}
\mathcal{L}_c = & \frac{1}{8} \theta_+(-\vec{q}, -\omega) \left[\frac{\omega^2 + \omega_{\vec{q}}^2}{V_+(q) + \frac{4\pi^2 \bar{\rho}}{m} \frac{1}{q^2}} \right] \theta_+(\vec{q}, \omega) \\
& + \frac{1}{8} \theta_-(-\vec{q}, -\omega) \left[\frac{\omega^2}{V_-(\vec{q})} + \frac{\bar{\rho}}{m} q^2 \right] \theta_-(\vec{q}, \omega) \\
& + \frac{\bar{\rho}}{4m} (\nu_1 - \nu_2) q^2 \theta_-(-\vec{q}, -\omega) \theta_+(\vec{q}, \omega)
\end{aligned} \quad (35)$$

where we safely dropped a linear derivative term in θ_- in Eqn. 23 in the Interlayer Coherent QH state. However, the linear derivative term will be shown to play important role in the incoherent disordered state in the next subsection. From Eqn.35, we can identify the three propagators:

$$\begin{aligned}
\langle \theta_+ \theta_+ \rangle &= \frac{\left(\frac{4m}{\bar{\rho}q^2}\right)(\omega^2 + v^2 q^2) \omega_q^2}{\omega^4 + \omega^2(\omega_q^2 + v^2 q^2) + f v^2 q^2 \omega_q^2} \\
\langle \theta_- \theta_- \rangle &= \frac{4V_-(q)(\omega^2 + \omega_q^2)}{\omega^4 + \omega^2(\omega_q^2 + v^2 q^2) + f v^2 q^2 \omega_q^2} \\
\langle \theta_+ \theta_- \rangle &= \frac{-4(\nu_1 - \nu_2)V_-(q)\omega_q^2}{\omega^4 + \omega^2(\omega_q^2 + v^2 q^2) + f v^2 q^2 \omega_q^2}
\end{aligned} \quad (36)$$

where $\omega_{\vec{q}}^2 = \omega_c^2 + \frac{\bar{\rho}}{m} q^2 V_+(q)$, the cyclotron frequency $\omega_c = \frac{2\pi\bar{\rho}}{m}$ and the spin wave velocity in the balanced case $v^2 = \frac{\bar{\rho}}{m} V_-(\vec{q})$ were defined before.

Performing the frequency integral of the first equation in Eqn.36 carefully, we find the the *leading term* of the equal time correlator of θ_+ stays the same as the balanced case Eqn.27:

$$\langle \theta_+(-\vec{q}) \theta_+(\vec{q}) \rangle = 2 \times \frac{2\pi}{q^2} + O\left(\frac{1}{q}\right) \quad (37)$$

which leads to the same algebraic order exponent 2 as in the balanced case Eqn.28.

We conclude that the algebraic order in the charge sector is independent of the imbalance. This maybe expected, because the total filling factor $\nu_T = 1$ stays the same.

In the $q, \omega \rightarrow 0$ limit, we can extract the leading terms of the $\theta_- \theta_-$ propergator:

$$\langle \theta_- \theta_- \rangle = \frac{4V_-(q)}{\omega^2 + f v^2 q^2} \quad (38)$$

where we can identify the spin wave velocity in the imbalanced case:

$$v_{im}^2 = f v^2 = 4\nu_1 \nu_2 v^2 = 4\nu_1(1 - \nu_1)v^2 \quad (39)$$

which shows that the spin-wave velocity attains its maximum at the balanced case and decreases parabolically as the im-balance increases. The corresponding KT transition temperature T_{KT} also decreases parabolically as the im-balance increases.

Similarly, in the $q, \omega \rightarrow 0$ limit, we can extract the leading terms in the $\theta_+ \theta_-$ propergator:

$$\langle \theta_+ \theta_- \rangle = \frac{-4V_-(q)(\nu_1 - \nu_2)}{\omega^2 + f v^2 q^2} = -(\nu_1 - \nu_2) \langle \theta_- \theta_- \rangle \quad (40)$$

which shows that the behavior of $\langle \theta_+ \theta_- \rangle$ is dictated by that of $\langle \theta_- \theta_- \rangle$ instead of $\langle \theta_+ \theta_+ \rangle$.

When the vortex excitations to be discussed in the following are included, the spin wave velocity will be renormalized down. As analyzed in detail in the last subsection, it is hard to incorporate the Lowest Landau Level (LLL) projection in the CB approach, so the spin wave velocity can only taken as a phenomenological parameter to be fitted to the microscopic LLL calculations or experiments. But we expect that the forms of all the propagators stay the same.

(2) Topological excitations

There are following 4 kinds of topological excitations: $\Delta\theta_1 = \pm 2\pi, \Delta\theta_2 = 0$ or $\Delta\theta_1 = 0, \Delta\theta_2 = \pm 2\pi$. Namely $(m_1, m_2) = (\pm 1, 0)$ or $(m_1, m_2) = (0, \pm 1)$. We can classify all the possible topological excitations in terms of (q, m_-) in the following table.

	$(1, 0)$	$(-1, 0)$	$(0, 1)$	$(0, -1)$
m_-	1	-1	-1	1
m_+	1	-1	1	-1
q	ν_1	$-\nu_1$	ν_2	$-\nu_2$

Table 2: The fractional charge in im-balanced case

The fractional charges in table 2 were determined from the constraint $\nabla \times \vec{a} = 2\pi\delta\rho$ and the finiteness of the energy in the charge sector:

$$\begin{aligned}
q &= \frac{1}{2\pi} \oint \vec{a} \cdot d\vec{l} = \frac{1}{2\pi} \times \frac{1}{2} \oint [\nabla\theta^+ + (\nu_1 - \nu_2)\nabla\theta^-] \cdot d\vec{l} \\
&= \frac{1}{2} [m_+ + (\nu_1 - \nu_2)m_-]
\end{aligned} \quad (41)$$

In contrast to the balanced case where q only depends on m_+ , q depends on m_+, m_- and the filling factors ν_1, ν_2 . Just like in balance case, any deconfined excitations with $(m_- = 0, m_+ = 2m)$ have charges $q = \frac{1}{2}m_+ = m$ which must be integers. While the charge of $(m_+ = 0, m_- = 2m)$ is $q = (\nu_1 - \nu_2)m$ which is charge neutral only at the balanced case.

The merons listed in table 2 are confined into the following two possible pairs at low temperature. (1) Charge neutral pairs: $(\pm\nu_1, \pm 1)$ or $(\pm\nu_2, \mp 1)$. They behave as bosons. The NGM will turn into charge neutral pairs at large wavevectors. (2) Charge 1 pair $(\nu_1, 1) + (\nu_2, -1)$ or charge -1 pair $(-\nu_1, -1) + (-\nu_2, 1)$. They behave as fermions. They are the lowest charged excitations in BLQH and the main dissipation sources for the charge transports. A duality transformation can be easily performed to express low energy physics in terms of the dynamics of these topological excitations. Performing the

duality transformation on Eqn.23 leads to the dual action in terms of the vortex degree of freedoms $J_\mu^{v\pm} = \frac{1}{2\pi}\epsilon_{\mu\nu\lambda}\partial_\mu\partial_\nu\theta_\pm = J_\mu^{v1} \pm J_\mu^{v2}$ and the corresponding dual gauge fields b_μ^\pm :

$$\begin{aligned}\mathcal{L}_d = & -i\pi b_\mu^+ \epsilon_{\mu\nu\lambda} \partial_\nu b_\lambda^+ - iA_{s\mu}^+ \epsilon_{\mu\nu\lambda} \partial_\nu b_\lambda^+ + i\pi b_\mu^+ J_\mu^{v+} \\ & + \frac{m}{2\bar{\rho}f} (\partial_\alpha b_0^+ - \partial_0 b_\alpha^+)^2 + \frac{1}{2} (\nabla \times \vec{b}^+) \cdot V_+(\vec{q}) (\nabla \times \vec{b}^+) \\ & - iA_{s\mu}^- \epsilon_{\mu\nu\lambda} \partial_\nu b_\lambda^- + i\pi b_\mu^- J_\mu^{v-} - h_z (\nabla \times \vec{b}^-) \\ & + \frac{m}{2\bar{\rho}f} (\partial_\alpha b_0^- - \partial_0 b_\alpha^-)^2 + \frac{1}{2} (\nabla \times \vec{b}^-) \cdot V_-(\vec{q}) (\nabla \times \vec{b}^-) \\ & - \frac{m}{\bar{\rho}f} (\nu_1 - \nu_2) (\partial_\beta b_0^- - \partial_0 b_\beta^-) (\partial_\beta b_0^+ - \partial_0 b_\beta^+) \quad (42)\end{aligned}$$

where $A_{s\mu}^\pm = A_{s\mu}^1 \pm A_{s\mu}^2$ are the two source fields. The last term can be shown to be irrelevant in the ILCQH state. The spin wave velocity in Eqn.39 can also be easily extracted from this dual action. Note that the spin (+ or -) sector of this dual action takes exactly the same form of 3D superconductor in an external magnetic field h_z .

It is constructive to compare this dual action derived from the CB approach with the action derived from MCF approach Eqn.8. We find the following three differences: (1) The topological vortex degree of freedoms $J_\mu^{v\pm}$ are missing in Eqn.8. These vortex degree of freedoms are needed to make the variable ϕ in Eqn.10 to be an angle variable $0 < \phi < 2\pi$. (2) The χ_+, χ_- terms in Eqn.8 are extra spurious terms. These extra spurious terms break $SU(2)$ symmetry even in the $d \rightarrow 0$ limit. (3) The linear term $-h_z(\nabla \times \vec{b}^-)$ is missing in Eqn.8. This linear term is not important in the interlayer coherent QH state, but it is very important in the in-coherent disordered state to be discussed in the following subsection. Indeed, if we drop all the χ_+, χ_- terms, use bare mass and also add the the topological vortex currents and the linear term by hands in Eqn.8, then Eqn.8 will be identical to We conclude that Eqn.42. Eqn. 23 and 42 from CB approach are the correct and complete effective actions.

We can also look at the static energy of a charge 1 meron pair consisting a meron with charge ν_1 and charge ν_2 separated by a distance R :

$$E_{mp} = E_{1c} + E_{2c} + \frac{\nu_1 \nu_2 e^2}{R} + 8\pi \nu_1 \nu_2 \rho_{s0} \ln \frac{R}{R_c} \quad (43)$$

where E_{1c}, E_{2c} are the core energies of meron 1 (charge ν_1) and meron 2 (charge ν_2) respectively, R_c is the core size of an isolated meron, $\rho_{s0} = \frac{\bar{\rho}}{8m}$ is the spin stiffness at the balanced case.

Minimizing E_{mp} with respect to R leads to an optimal separation: $R_o = \frac{e^2}{8\pi \rho_{s0}}$ which, remarkably, is independent of the imbalance. Namely, the optimal separation of a meron pair remains the same as one tunes the imbalance. Plugging R_o into Eqn.43 leads to the optimal energy of a meron pair:

$$E_o = E_{1c} + E_{2c} + \nu_1 (1 - \nu_1) \left(\frac{e^2}{R_o} + 8\pi \rho_{s0} \ln \frac{R_0}{R_c} \right) \quad (44)$$

Because of logarithmic dependence on R_c , we can neglect the ν_1 dependence in R_c , then the second term in Eq.44 decreases parabolically as im-balance increases. Unfortunately, it is hard to know the ν_1 dependence of E_{1c}, E_{2c} and R_c from an effective theory, so the dependence of the energy gap E_o on ν_1 is still unknown.

C. Im-balance driven quantum phase transition

So far, the discussions are in the ILCQH state, now we will study the incoherent disordered state when the distance is only slightly larger than d_{c1} . We assume the following physical picture in the whole distance range: For balanced BLQH, there are two critical distances $d_{c1} < d_{c2}$ (Fig.2).

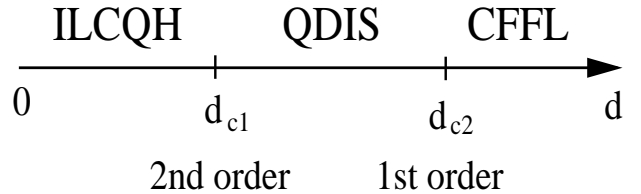


Fig 2: The phase diagram as the distance between the two layers increases

When $0 < d < d_{c1}$, the system is in the interlayer coherent QH state (ILCQH), when $d_{c1} < d < d_{c2}$, the system is in the quantum disordered insulating state (QDIS), there is a second order transition at d_{c1} driven by the quantum fluctuation. We assume that Eqn.23 and its dual action Eqn.42 work on both sides until $d < d_{c2}$. When $d_{c2} < d < \infty$, the system becomes two weakly coupled $\nu = 1/2$ Composite Fermion Fermi Liquid (CFFL) state. There is a first order transition at $d = d_{c2}$. In ILCQH state, there is a QH charge gap in the charge sector but gapless in the spin sector. While in QDIS, there is a Mott charge gap in the charge sector and a spin gap in the spin sector also. There are charges gaps on both sides although with completely different origins, the charge gap vanishes only at the quantum critical point (QCP) at d_{c1} . Although there are very little dissipations in both the ILCQH and CFFL, we expect to see strong enhancement of drag and dissipations in the QDIS which is consistent with the recent experimental findings in [32]. The experimental observations that both zero voltage tunneling peak [4] and the Hall drag resistivity [5] develop very gradually when $d \sim d_{c1}$ also suggest the transition at $d = d_{c1}$ is a 2nd order phase transition.

On both sides of the QCP, because there are charge gaps, we can integrate out the charge sector and focus on the effective action in the spin sector:

$$\mathcal{L}_s = \frac{i}{2} \delta\rho^- \partial_\tau \theta^- + \frac{\bar{\rho}f}{2m} \left(\frac{1}{2} \nabla \theta_- \right)^2 + \frac{1}{2} \delta\rho^- V_-(\vec{q}) \delta\rho^- - h_z \delta\rho^- \quad (45)$$

where the im-balance field h_z couples to the conserved quantity $\delta\rho^-$. As mentioned in the previous section, although the $-h_z \delta\rho^-$ term is irrelevant in the ILCQH state, it plays important role in the QDIS to be discussed in the following.

Integrating out $\delta\rho^-$ leads to

$$\mathcal{L}_s = \frac{1}{2V_-(\vec{q})} \left(\frac{1}{2} \partial_\tau \theta^- + ih_z \right)^2 + \frac{\bar{\rho}f}{2m} \left(\frac{1}{2} \nabla \theta_- \right)^2 \quad (46)$$

where $h_z = V_- \bar{\rho}(\nu_1 - \nu_2)$ plays the role of the *time* component of *imaginary* gauge field.

The model Eqn.46 was studied extensively in Refs. [33,34]. It was also shown to be dual to a superconductor in an external magnetic field [35]. The phase diagram in boson and dual picture is shown in Fig.3.

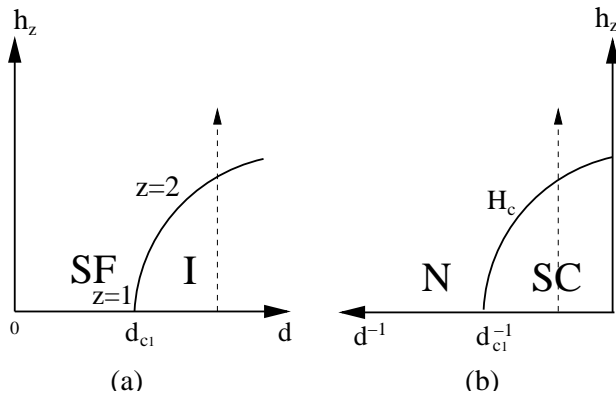


Fig 3: The phase diagram in the boson picture Eqn.47 (a) and in the dual picture Eqn.48 of Type I superconductors (b). (SF) is the superfluid phase, (I) stands for Insulating phase. (SC) stands for the Meissner phase of a superconductor, (N) stands for a normal phase

Fig. 3a shows that when $h_z = 0, d > d_{c1}$, the system is in the QDIS. Increasing the im-balance (along the dashed line in Fig.3) will drive the system back into the ILCQH. The transition is a zero density transition of dynamic exponent $z = 2$ driven by chemical potential described by the effective action:

$$\mathcal{L} = \Psi^*_-(\vec{x}, \tau) \hbar \partial_\tau \Psi_-(\vec{x}, \tau) - \Psi^*_-(\vec{x}, \tau) \frac{\hbar^2 \nabla^2}{2m} \Psi_-(\vec{x}, \tau) - \mu |\Psi_-(\vec{x}, \tau)|^2 + u |\Psi_-(\vec{x}, \tau)|^4 + \dots \quad (47)$$

where the chemical potential $\mu = h_z - \Delta$ and Δ is the pseudo-spin gap in the QDIS. This transition is in a different universality class than the interaction driven $z = 1$ 3D XY transition at $h_z = 0$. Fig.3 also implies that d_c increases as h_z increases. At the quantum critical point $\mu = 0, h_z = \Delta \sim (d - d_{c1})^{z\nu}$. At mean field theory, $\nu = 1/2$, then $h_z^2 = d - d_{c1}$. For 3 D XY model,

$z = 1, \nu \sim 0.7, h_z^2 = (d - d_{c1})^{1.4}$, hence $\frac{dh_z}{dd}|_{d_{c1}}$ diverges as shown in Fig.3. The scaling function of the magnetization $M = \delta\rho_- = \langle \Psi_-^* \Psi_- \rangle$ as a function of the chemical potential μ and the temperature T was also derived in [34].

By a duality transformation [35], Eqn.47 can be mapped to a 3D superconductor in an external magnetic field h_z .

$$\mathcal{L}_d = \frac{|(\partial_\mu - ib_\mu^-) \Phi_-(x)|^2}{2m} + a |\Phi_-(x)|^2 + b |\Phi_-(x)|^4 + \frac{1}{8\pi} B_-^2 - h_z \cdot B_- \quad (48)$$

where $x = (\vec{x}, \tau)$ and $B_- = \nabla \times \vec{b}_-$. As noted below Eqn.42, the spin (+ or -) sector of the dual action Eqn.42 takes exactly the same form. In the duality transformation, the (SF) phase is mapped to the (N) phase, while the (I) phase is mapped to (SC) phase. When h_z exceeds the critical field H_c , there is a transition from (SC) to (N) as shown in Fig.3b.

Although only short-range interactions are encoded in the long-wave length effective actions Eqn.47 and 48, there is a long-range interaction $V_-(\vec{q})$ in Eqn.45 between the dilute bosons in Fig.3a or the vortices in Fig.3b, because $V_-(r) = \frac{1}{r} - \frac{1}{\sqrt{r^2 + d^2}} \sim \frac{d^2}{2r^3}$ if $r \gg d$. The long-range interaction between the bosons will stabilize a density wave state in the boson picture (Fig. 4a) or transforms a superconductor from type I to type II (Fig. 4b).

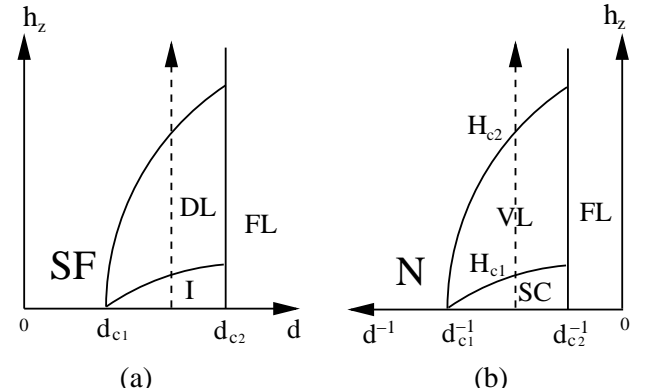


Fig 4: The phase diagram of model Eqn.46 in boson picture (a) and dual picture of Type II superconductors. The new intermediate phase is a Dipolar Lattice (DL) state in the boson picture (a) and a Vortex Lattice (VL) state in Type II superconductors (b). When $d > d_{c2}$, the imbalance will not be able to transfer the CFFL state back to the ILCQH state. The line at d_{c2} could also depend on the imbalance.

In the spin sector, the charge quantization in the boson picture or flux quantization in the dual picture dictates $\delta\rho_- = 1$. In the charge sector, the simplest configuration is $\delta\rho_+ = 0$, because the total charge remains constant

during the charge transfer from the top layer to the bottom layer. This is a density wave state of electric dipoles whose charge distribution is shown in Fig. 5:

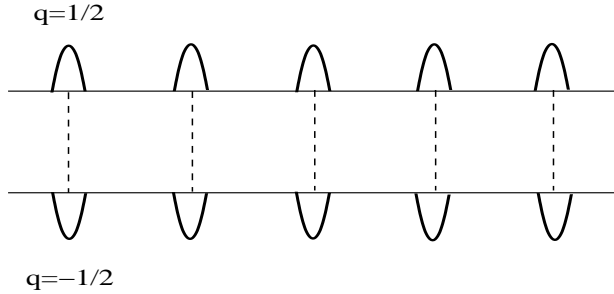


Fig. 5: The charge distribution of the Dipolar Lattice (DL) state in both layers. The charge bump in top layer carries charge $1/2$, while that directly below in the bottom layer carries charge $-1/2$.

From Fig. 5, we can see that the static electric dipoles in this DL state interact with each other with the long-range $\frac{d^2}{4r^3}$ dipole-dipole interaction. The crystal structure of this DL state is likely to be a triangular lattice, but other lattice structures or stripe structure are also possible. It is important to distinguish the charge bumps in the DL state from the meron excitations in the ILCQH state: the DL state is a quantum disordered state where the magnitude $\delta\rho_-$ is fixed, the phase θ_- fluctuates. It is a *ground* state at finite imbalance with long range position order. The charge bumps carry no total charges $\delta\rho_+ = 0$, but relative charge $\delta\rho_- = 1$. They behave as bosons. While ILCQH state is an ordered state where the phase θ_- is fixed, the magnitude $\delta\rho_-$ fluctuates. In this state, an electron in one layer and a hole in another layer form an exciton which condenses into the superfluid. The excitations above the ILCQH ground state are called merons which carry total fractional charges $\pm\nu_1, \pm\nu_2$ as shown in Table 2 at finite imbalance. The charge neutral meron pairs behave as bosons, while charge ± 1 behave as fermions.

In Fig.4, there are three phases and two quantum phase transitions as we crank the imbalance at $d > d_{c1}$ along the dashed line in Fig.4. (A) when we increase the voltage bias $0 < V < H_{c1}$, the QDIS stays untouched and the imbalance $h_z = \bar{\rho}_1 - \bar{\rho}_2$ is locked at zero. (B) when we increase the voltage bias further $H_{c1} < V < H_{c2}$, the QDIS gets into the DL and the imbalance $h_z > 0$ starts to increase also. This vortex lattice state is still an insulating state. which has both a Mott charge gap and a spin gap. The Bi-layer system accommodates the charge imbalance in the form of the DL state whose charge distribution between the two layers is shown in Fig.5. (C) As we increases the voltage bias even further $V > H_{c2}$, the DL state melts into the ILCQH state and the imbalance h_z continues to increases. In the ILCQH, there is a QH charge gap, but gapless in the spin sector, the ex-

citons which is a bound state of an electron in one layer and a hole in another layer condense and form superfluid. There are spin waves and topological excitations above the exciton condensate as classified in the previous sections. We have charge gaps on both sides of the curve $h_z = H_{c2}$, although with different origins, the charge gap vanishes only along the curve. Due to these low energy charge fluctuations, the quantum critical behavior along the curve is still unknown. Recent experiment [40] found a parabolic behavior $h_z^2 \sim d - d_{c0}$ which looks like a mean field behavior with $z = 1, \nu = 1/2$. This mean field like behavior remains to be explained. Of course, if we increases the bias voltage V to a very large value, all the charges will move into one layer, the system will evolve into a SLQH regime. In SLQH limit, Eqn.23 is not valid anymore, this limit can not be addressed in this paper.

When the distance of the two layers is further increased to larger than a second critical distance d_{c2} , then all the signature of the interlayer coherent state are lost. The flux attachment transformation shown in Eqn.2 which treats the electrons in the two layers at the same footing completely breaks down and a completely different flux attachment transformation within a single layer to transform an electron into a Composite Fermion Eqn.5 must be used [23]. When $d > d_{c2}$, the two layers are decoupled into two separate $\nu = 1/2$ CF Fermi liquid state (Fig.2). We expect that there is a level crossing and associated first order transition at d_{c2} . This quantum phase transition is not addressed in this paper and remains an interesting open question. Obviously, when $d > d_{c2}$, increasing the bias voltage will not transform the two decoupled FL state back into the ILCQH state. The line at $d = d_{c2}$ in Fig. 4 is likely to bend to the left. At $d < d_{c1}$, it is the composite boson to feel zero field, they are condensed into the ILCQH, while at $d > d_{c2}$, it is the composite fermion to feel zero field, they form a Fermi surface. There can only be a first order transition between these two limits.

It was also argued [11,39] that the disorder may play important roles even inside the ILCQH phase. We expect it to change the universality class at the QCP. For example, it may split the one QCP into two QCPs and introduce a gauge glass like phase just like bose glass phase in the dirty boson case studied in [33]. In the presence of disorder, the DL state may also become a glassy phase like Dipolar Glass (DG) state where only short range of crystalline order should survive. The disorder may also smear the first order transition at d_{c2} into a 2nd order transition.

Fig. 2, 3, 4, 5 are valid only for small imbalance such that ν_1, ν_2 do not fall into fractional Quantum Hall plateaus for separate layers. For large imbalance such as two layers with $\nu_1 = 1/3, \nu_2 = 2/3$ still with $\nu_T = 1$, then the two weakly coupled layers show $\nu_1 = 1/3$ and $\nu_2 = 2/3$ fractional Quantum Hall states separately when $d > d_{c2}$. Because there are intralayer gaps, they are more

robust against the interlayer correlations, we expect d_{c2} for $\nu_1 = 1/3, \nu_2 = 2/3$ to be *smaller* than $\nu_1 = \nu_2 = 1/2$. If we bring them closer, there could be a direct 1st order transition at $d_{c1} = d_{c2}$ from the weakly coupled pair to the ILCQH, or through a very narrow regime of QDIS.

D. Interlayer tunneling

Note that in contrast to MCF, the same phase factor appears in the singular gauge transformation Eqn.18 for the two layers $a = 1, 2$ which get canceled exactly in H_t :

$$\begin{aligned} H_t &= t\phi_1^\dagger(\vec{x})\phi_2(\vec{x}) + h.c. = 2t\sqrt{\bar{\rho}_1\bar{\rho}_2}\cos(\theta_1 - \theta_2) \\ &= 2t\bar{\rho}\sqrt{\nu_1\nu_2}\cos\theta_- \end{aligned} \quad (49)$$

In the presence of in-plane magnetic field $B_{||} = (B_x, B_y)$, the effective Lagrangian is:

$$\begin{aligned} \mathcal{L}_s &= \frac{1}{2V_-(\vec{q})}(\frac{1}{2}\partial_\tau\theta^- + ih_z)^2 + \frac{\bar{\rho}}{2m}\nu_1\nu_2(\nabla\theta_-)^2 \\ &+ 2t\bar{\rho}\sqrt{\nu_1\nu_2}\cos(\theta_- - Q_\alpha x_\alpha) \end{aligned} \quad (50)$$

where $x_\alpha = (x, y)$, $Q_\alpha = (-\frac{2\pi dB_y}{\phi_0}, \frac{2\pi dB_x}{\phi_0})$.

In balanced case, it was found that when the applied in-plane magnetic field is larger than a critical field $B > B_{||}^* \sim (t_0/\rho_{s0})^{1/2}$, there is a phase transition from a commensurate state to an incommensurate state with broken translational symmetry. When $B > B_{||}^*$, there is a finite temperature KT transition which restores the translation symmetry by means of dislocations in the domain wall structure in the incommensurate phase.

As can be seen from Eq.50, $\rho_s \sim \nu_1\nu_2$, while $t \sim \sqrt{\nu_1\nu_2}$, so the critical field $B_{||}^* \sim (t/\rho_s)^{1/2} \sim (\nu_1\nu_2)^{-1/4}$ increases as one tunes the im-balance.

E. Comparison with the earlier work

In this section, I assumed that for balanced BLQH, there are two critical distances $d_{c1} < d_{c2}$. When $0 < d < d_{c1}$, the system is in the interlayer coherent QH state (ILCQH), when $d_{c1} < d < d_{c2}$, the system is in the quantum disordered insulating state (QDIS), there is a second order transition at d_{c1} driven by the quantum fluctuation. When $d_{c2} < d < \infty$, the system becomes two weakly coupled $\nu = 1/2$ Composite Fermion FL (CFFL) state. There is a first order transition at $d = d_{c2}$. From this picture, I predicted that when $d_{c1} < d < d_{c2}$, applying bias voltage across the two layers will drive the system back into ILCQH state. Particularly, we find there are two quantum phase transitions from the QDIS to a novel DL phase and then to the ILCQH as we increase the imbalance. Although the ILCQH phase and FL phase at the two extreme distances are well established, the picture of how the ILCQH evolves into the two weakly-coupled FL

states is still not clear, namely, the nature of the intermediate phase at $d_{c1} < d < d_{c2}$ is still under debate. There are other proposals except the one proposed in this paper. By the microscopic LLL+ HF approach, the authors in [36–38] claimed that the transition at d_{c1} is a instability to a quantum disordered pseudospin density wave state driven by the gap closing of magneto-roton minimum at a finite wave-vector. They predicted that on the ordered side, the imbalance increases the spin stiffness, on the disordered side, the imbalance drives a quantum phase transition from the disordered state to the ILCQH. But the properties of the disordered phase and the associated quantum phase transition were not discussed in [36–38]. The Phase (A) in Fig.4 is not shown in [36–38,40] where the phase diagram was drawn against fixed charge imbalance instead of fixed bias voltage (or chemical potential difference between the two layers). As stated in the previous sections, the advantage of this microscopic LLL+HF approach over the CB approach used in this paper is that the calculations were performed explicitly in the LLL. However, in this LLL+HF approach, the charge fluctuations are completely integrated out, therefore can not address the interplay between the QH effects in the charge sector and the interlayer phase coherence in the spin sector. It was shown in section B that in the imbalanced BLQH, there is a coupling between the charge sector and the spin sector even when ignoring all the topological excitations. This coupling renormalizes down the spin-wave velocity. As stated in section C, the charge sector also becomes gapless at d_{c1} , so its fluctuation can not be ignored near d_{c1} . However, as pointed out in the introduction and section A, it is hard to incorporate the LLL projection. Some parameters can only be calculated in the LLL+HF approaches. So the CB approach in this paper and the microscopic LLL+HF approach in [37] are complementary to each other.

IV. CONCLUSIONS

Three common approaches to SLQH systems are the wavefunction (or first quantization) [41,21], Composite Fermion Field Theory (CFFT) [22–24] and Composite Boson Field Theory (CBFT) approaches [27,28]. The Composite Fermion Wavefunction (CFW) [21] approach has been quite successfully applied to study SLQH at Jain's series at $\nu = \frac{p}{2sp \pm 1}$. CFFT has been successfully used to study the CF Fermi liquid at $\nu = 1/2$ which is at the end point of Jain's series in the limit $p \rightarrow \infty$. However, there are some problems with CFFT approach whose equivalence to the CFW is still not obvious even in SLQH. These problems have been vigorously addressed in [24]. CBFT approach has so far only limited to Laughlin's series $\nu = \frac{1}{2s+1}$ which is only a $p = 1$ subset of Jain's series. It can not be used in any simple way to study $p > 1$ Jain series and $\nu = 1/2$ CF Fermi liquid.

But it has also been applied successfully in $\nu = 1$ spin-unpolarized QH systems [29]. In this paper, we used both CFFT and CBFT approach to study the im-balanced BLQH systems. We found that CBFT approach is superior than CFFT approach in the BLQH with broken symmetry. We also pushed the CBFT theory further to study the incoherent disordered side and quantum phase transitions between different ground states.

In the first part of this paper, we used a MCF approach to study im-balanced BLQH systems. We achieved some success, but also run into many troublesome problems. We explicitly identified these problems and motivated the alternative CB approach. Extension of Murthy-Shankar's formalism [24] in SLQH to BLQH can not fix these problems. In the second part of the paper, we developed a simple and effective CB theory to study the BLQH. The CB theory naturally fixed all the problems suffered in the MCF theory presented in the first part. By using this CB theory, we are able to put spin and charge degree freedoms in the same footing, explicitly brought out the spin-charge connection in a straightforward way and classified all the possible excitations in a systematic way. By using this CB theory, we first studied the balanced BLQH and re-derived many previous results in a simple and transparent way. We made detailed comparisons between the spin sector of the CB theory with EPQFM derived from microscopic LLL approach. We found that although some parameters in the spin sector can only be taken as phenomenological parameters, the functional form is identical to the EPQFM. We then applied the theory to study the effects of imbalance on both the ordered side and the disordered side and achieved some new results. We found that on the ordered side, as we tune the im-balance, the system supports continuously changing fractional charges, the spin-wave velocity decreases quadratically, while the meron pair separation remains the same and the critical in-plane magnetic field for the C-IC transition increases. We also derived the dual action of the CB theory in terms of topological currents and dual gauge fields. By comparing this dual action with the action derived from MCF theory, we can explicitly identify the missing and the artifacts of the MCF approach. On the disordered side, we studied the quantum phase transition from in-coherent disordered state to the interlayer coherent state. We find there are two quantum phase transitions, the first one is essentially a zero density transition from the incoherent disordered state to a novel DL state driven by the Bose condensation induced by the imbalance, the second one is from the DL state to the interlayer coherent QH state. We discussed briefly the effects of disorders. We also compared our results with the previous results from LLL+HF approach and available experimental data.

Only the interlayer coherent (111) state was discussed in this paper, it can be easily generalized to other interlayer coherent (m, m, m) (with m odd) states at total

filling factors $\nu_T = 1/m$. For general (m, m', n) states with m, m' are odd and $mm' - n^2 \neq 0$, because there are no broken symmetry in the ground states and no associated gapless Goldstone modes, we expect the Composite Fermion approach works better. For example, $(3, 3, 1)$ state at $\nu_T = 1/2$ can be described in terms of the Entangled Composite Fermion (ECF) discussed at section II 7.

It is general true that when there is an ordered state with broken symmetry and an associated order parameter, bosonic approach is superior than fermionic approach. For example, in Quantum Antiferromagnet, fermionic approach can only address the disordered phase [42], while bosonic approach [43] can address not only the disordered phase, but also the ordered phase with broken symmetry and the quantum phase transition between the disordered phase and ordered phase. Similarly, in quantum spin glass, bosonic approach can study spin liquid, spin glass and the quantum phase transition between the two, while the fermionic representation can only study the spin liquid phase [44]. In SLQH system, there is only algebraic long range order, but no broken symmetry and no true ordered state, so CF approach could be very successful. While (m, m, m) BLQH system has a true broken symmetry ground state and an associated order parameter and a Goldstone mode, the CB approach becomes more effective as demonstrated in this paper.

I thank J. K. Jain for many insightful discussions. I also thank H. Fertig, E. Fradkin, S. M. Girvin, B. Halperin, A. H. Macdonald and G. Murthy for helpful discussions.

[1] B. I. Halperin, *Helv. Phys. Acta* 56, 75 (1983); *Surf. Sci.* 305, 1 (1994)
[2] For reviews of bilayer quantum Hall systems, see S. M. Girvin and A. H. Macdonald, in *Perspectives in Quantum Hall Effects*, edited by S. Das Sarma and Aron Pinczuk (Wiley, New York, 1997).
[3] J. P. Eisenstein, L. N. Pfeiffer and K. W. West, *Phys. Rev. Lett.* 69, 3804 (1992); Song He, P. M. Platzman and B. I. Halperin, *Phys. Rev. Lett.* 71, 777 (1993).
[4] I. B. Spielman *et al*, *Phys. Rev. Lett.* 84, 5808 (2000). *ibid*, 87, 036803 (2001).
[5] M. Kellogg, *et al*, *Phys. Rev. Lett.* 88, 126804 (2002).
[6] H. Fertig, *Phys. Rev. B* 40, 1087 (1989).
[7] X. G. Wen and A. Zee, *Phys. Rev. Lett.* 69, 1811 (1992).
[8] Z. F. Ezawa and A. Iwazaki, *Phys. Rev. B*, 47, 7259; 48, 15189 (1993). *Phys. Rev. Lett.* 70, 3119 (1993).
[9] Kun Yang *et al*, *Phys. Rev. Lett.* 72, 732 (1994). *Phys. Rev. B* 54, 11644 (1996).
[10] K. Moon *et al*, *Phys. Rev. B* 51, 5138 (1995).
[11] L. Balents and L. Radzihovsky, *Phys. Rev. Lett.* 86, 1825 (2001). A. Stern, S. M. Girvin, A. H. Macdonald and N.

Ma, *ibid* 86, 1829 (2001). M. Fogler and F. Wilczek, *ibid* 86, 1833 (2001).

[12] A. López and E. Fradkin, Phys. Rev. B 51, 4347 (1995); *ibid*, 63, 085306, 2001. See also a review article by the two authors in *Composite Fermions: A unified view of the Quantum Hall Regime*, edited by Olle Heinonen. World Scientific (Singapore, 1998).

[13] Yong Baek Kim *et al*, cond-mat/0011459.

[14] M. Y. Veillette, L. Balents and M. P. A. Fisher, Phys. Rev. B, 66, 155401 (2002).

[15] V. W. Scarola and J. K. Jain, Phys. Rev. B 64, 085313 (2001).

[16] P. W. Anderson, cond-mat/9812063.

[17] Jinwu Ye, Phys. Rev. Lett. 86, 316 (2001).

[18] L. Balents, M. P. A. Fisher and C. Nayak, Int. J. Mod. Phys. B12, 1033(1998), Phys. Rev. B60, 1654 (1999).

[19] Jinwu Ye, Phys. Rev. Lett. 87, 227003 (2001); Phys. Rev. B, 65, 214505 (2002).

[20] The concept of MCF was implied previously in [7,12,15] in different languages. Here, we explicitly write down the relation between a MCF and an original electron by Eqn.2 which is useful to the following developments in the paper.

[21] J. K. Jain, Phys. Rev. Lett. 63, 199 (1989).

[22] A. Lopez and E. Fradkin, Phys. Rev. B, 44, 5246 (1991).

[23] B. I. Halperin, P. A. Lee and N. Read, Phys. Rev. B47, 7312 (1993).

[24] See the review by G. Murthy and R. Shankar, Rev. of Mod. Phys. 75, 1101, 2003.

[25] Jinwu Ye and S. Sachdev, Phys. Rev. Lett. 80, 5409 (1998). Jinwu Ye, Phys. Rev. B60, 8290 (1999).

[26] M. Peskin, Ann. Phys. 113, 122 (1978); C. Dasgupta and B. I. Halperin, Phys. Rev. Lett. 47, 1556 (1981).

[27] S. M. Girvin and A. H. Macdonald, Phys. Rev. Lett. 58, 1252 (1987).

[28] S. Z. Zhang, T. H. Hansson and S. Kivelson, Phys. Rev. Lett. 62, 82 (1989). S. Z. Zhang, Int. J. Mod. Phys. B 6, 25 (1992).

[29] S. L. Sondhi *et al*, Phys. Rev. B 47, 16419 (1993).

[30] Jinwu Ye and Gun Sang Jeon, cond-mat/0407258.

[31] For discussions on relations between Abelian bosonization and Non-Abelian bosonization approaches to multi-channel Kondo model, see Jinwu Ye, Phys. Rev. Lett. 77, 3224 (1996).

[32] M. Kellogg, *et al*, Phys. Rev. Lett. 90, 246801 (2003).

[33] M. P. A. Fisher, P. B. Weichman, G. Grinstein and D. S. Fisher, Phys. Rev. B 40, 546 (1989).

[34] S. Sachdev, cond-mat/9312018, S. Sachdev, T. Senthil and R. Shankar, Phys. Rev. B 50, 258 (1994).

[35] M. P. A. Fisher and D. H. Lee, Phys. Rev. B 39, 2756 (1989).

[36] C. B. Hanna, Bull. Am. Phys. Soc. 42, 553 (1997)

[37] Y. N. Joglekar and A. H. Macdonald, Phys. Rev. B 65, 235319 (2002).

[38] W. R. Clarke, *et. al*, preprint

[39] J.P. Eisenstein and A.H. MacDonald, cond-mat/0404113. M. Kellogg, *et al*, cond-mat/0401521. E. Tutuc, M. Shayegan, D.A. Huse, cond-mat/0402186.

[40] I.B. Spielman, *et al*, cond-mat/0406067.

[41] Laughlin, in *The Quantum Hall Effects*, 2nd ed. edited by R. E. Prange and S. M. Girvin (Springer-Verlag, New York, 1990).

[42] I. Affleck and J. B. Marston, Phys. Rev. B 37, 3774 (1988).

[43] N. Read and S. Sachdev, Phys. Rev. B 42, 4568 (1990).

[44] S. Sachdev and Jinwu Ye, Phys. Rev. Lett. 70, 3339 (1993).